Low Loss HEMA/EMA Copolymer Waveguides with a Range of Wetting and Optical Properties

D. S. WALKER, K. BALASUBRAMANIAN, and W. M. REICHERT*

Department of Biomedical Engineering, Duke University, Durham, North Carolina 27706

SYNOPSIS

Homopolymers and copolymers of optical grade hydroxyethyl methacrylate (HEMA) and ethyl methacrylate (EMA) were synthesized with bulk copolymer compositions of 0, 10, 43, 75, 86, 89, and 100 mol % HEMA. Attenuated total reflection IR (ATR-IR) and X-ray photoelectron (XPS) spectroscopies showed an unhydrated surface composition that varied insignificantly from the bulk. Polymer surface wettability, percent swelling of the copolymers in water, and the bulk refractive index increased with increasing HEMA content. High-quality thin-film integrated optical waveguides (IOW) were spun cast from copolymer solutions with propagation losses of < 1 dB/cm. Waveguide refractive indices determined from coupling angle measurements agreed closely with the bulk measurements. These results show that HEMA/EMA copolymers that form transparent films produce polymer IOWs with a range of bulk swellabilities, surface wettabilities, and optical densities. © 1993 John Wiley & Sons, Inc.

INTRODUCTION

Acrylics are a class of optically transparent polymers with good film forming properties.[1] Cross-linked copolymers of polar and nonpolar acrylic monomers produce hydrogels that have found broad biomaterial applications ranging from soft contact lenses[2] to controlled drug delivery systems[3] to surface modifications of implant materials.[4] Acrylic biomedical hydrogels are typically a copolymer of hydroxyethylmethacrylate (HEMA) with either methylmethacrylate (MMA) or ethylmethacrylate (EMA).[5]

HEMA and EMA are structurally homologous acrylics with HEMA possessing a pendant polar hydroxyl group that imparts a degree of water solubility (Fig. 1). Free radical polymerization of HEMA and EMA over a range of monomer feed ratios (x and y in Scheme 1) form a random copolymer series with a well-documented range of surface energies.[6] HEMA/EMA copolymers have been used extensively by Horbett et al. to study the influence of polymer surface energy on cell[7] and platelet adhesion[8] and protein adsorption.[9] As evidenced by the optical clarity of soft contact lenses, acrylic hydrogels may be useful for producing optical devices modulated by interactions with molecules in aqueous media. Key steps in this direction are determining whether films of HEMA/EMA can be made of sufficient quality to efficiently guide light and whether such devices can assay molecular phenomena at the polymer/solution interface.

This paper addresses the first point by presenting the fabrication and characterization HEMA/EMA thin-film integrated optical waveguides (IOWs) with a range of surface wettabilities, bulk swellabilities, and refractive indices. Elsewhere, we show that the dB/cm loss of these waveguides can be modulated quantitatively by protein adsorption to the polymer/solution interface.[10] The detailed optical theory pertinent to polymer thin-film IOWs are available,[11] as are discussions of their fabrication.[12] Although polymethylmethacrylate (PMMA) is a common material for polymer waveguide fabrication,[13] to our knowledge no one has attempted to produce waveguides from either HEMA, EMA, or their copolymers.

Briefly, an IOW is an approximately micron-thick transparent film of higher refractive index (n_2) than

* To whom correspondence should be addressed.

Journal of Applied Polymer Science, Vol. 49, 2147–2155 (1993)
 CCC 0021-8995/93/122147-09

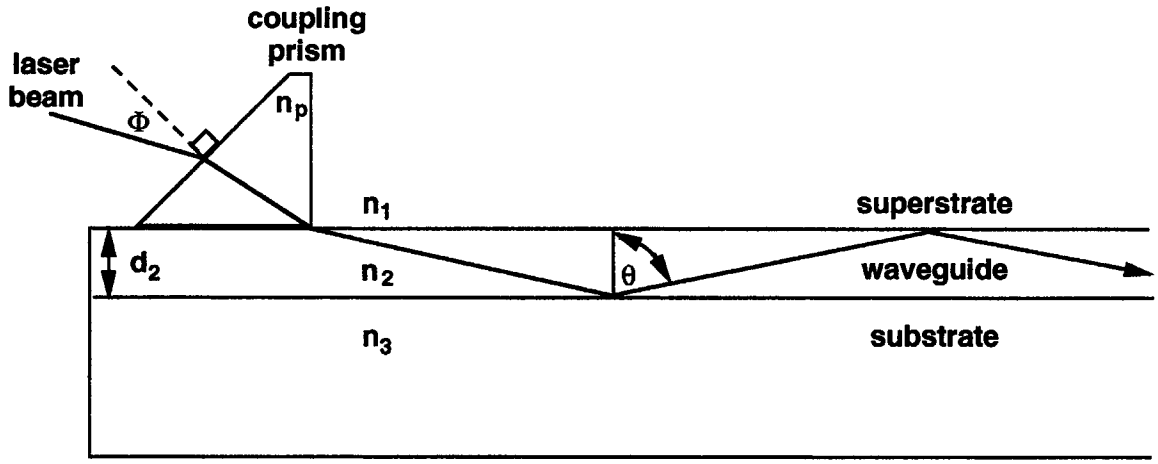

Figure 1 Schematic illustration of a thin-film IOW showing a ray tracing representation of a prism-coupled guided mode. Note that light is incoupled at the angle ϕ and propagates at the angle θ.

the surrounding superstrate (n_1) and substrate (n_3). Light coupled into the waveguide (usually by a high refractive index prism) propagates by repeated total internal reflection down the film, but only at a discrete set of propagation angles (θ) called guided modes (Fig. 1); for example, a 1-μm thick polymer film on a glass microscope slide will have 1–3 guided modes with approximately 1000 internal reflections per cm. Consequently, the guided mode of an IOW appears macroscopically as a continuous streak of light confined within the waveguiding film.

EXPERIMENTAL

Polymer Fabrication

A copolymer series of HEMA (130.14 g/mol, Optical Monomer) and EMA (114.15 g/mol, Fluka) was fabricated by thermally initiated free-radical polymerization of dilute monomer solutions. The monomers obtained were of optical quality and no further purification was performed. Monomer feed ratios (HEMA/EMA) of 0/10, 1/9, 2/8, 4/6, 6/4, 8/2, and 10/0 were used to obtain a good range of copolymer compositions. Reaction mixtures consisted of 4 mL monomer in 36 mL ethanol for all HEMA containing monomer mixtures, or 36 mL toluene for the all EMA monomer mixture, and 0.1% (w/w) of the thermal initiator 2,2′-azobis[2-methylpropionitrile] (AIBN, Kodak). Solutions were sealed, degassed for a half hour with 99.999% pure nitrogen, and then placed in a 60°C water bath for 12 h. Polymer was precipitated in an excess of hexane, dried overnight to remove excess solvent, and percentage yields were calculated. A more detailed description of the HEMA/EMA polymerization is available.[14]

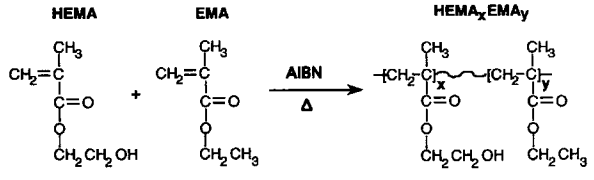

Scheme 1. Chemical structure of HEMA and EMA monomers and their copolymers.

Sample Preparation

Surface analysis of the copolymer series was conducted on thin polymer films applied to appropriate substrates for the technique used. Thin films were fabricated by spin coating or solvent casting on solid substrates. Except for the Wilhelmy plate measurements, 8–10% solutions of polymer were passed through a 0.45-μm syringe filter and applied to the substrate surface, followed by oven drying at 60°C overnight to remove residual solvent. Initial attempts at film formation according to Horbett et al.[15] (methanol for HEMA rich polymers and chlorobenzene EMA rich polymers) produced films with an unacceptable level of phase separation, surface irregularity, and cloudiness. The solvent system used for the films analyzed in this paper was dimethyl formamide (DMF) for the polymers with HEMA-rich monomer feeds and a mixture of isobutanol/toluene corresponding to the HEMA/EMA monomer feed ratio for the remainder. It was found that these solvents formed defect free, macroscopically

smooth, and optically clear thin films when spun and dip cast. The 89 mol % HEMA copolymer was not used in many of the measurements because the other six polymers provided a good range of monomer compositions.

Infrared Spectroscopy

Mol % HEMA composition of the polymers was determined using IR spectroscopy from the ratio of the hydroxyl band (3580 cm^{-1}) of HEMA and the carbonyl band (1700 cm^{-1}) possessed by both monomers. All values of the measured OH/C=O band ratio were normalized to the HEMA homopolymer that was assigned a value of 1.0. Transmission IR was used to sample the bulk composition. Attenuated total reflection (ATR)-IR was used to sample the copolymer to a depth of approximately 6000 Å. Transmission IR was performed on copolymer coated KBr plates in a Perkin–Elmer 783 grating IR spectrometer. ATR-IR was performed using copolymer coated Ge crystals in a Bio-Rad FTS-60A Fourier transform IR spectrometer. A total of 256 scans at 8 cm^{-1} resolution were collected and the spectra were background corrected using manufacturer supplied software.

Refractometry

Bulk refractive index values were determined using a Bausch and Lomb Abbe-3L refractometer. Polymer samples were solvent cast on the sample crystal, air dried, and three measurements were made for each sample.

Bulk Swelling

Three small dried pieces of each copolymer were weighed on a Metler AE166 balance and then submerged in water at room temperature and allowed to swell. All samples were removed at 1 and 24 h, dabbed with a Kimwipe to remove any surface drops, and weighed. Percent swelling, or percent water gain, was calculated by determining weight gain of the sample. Average values are reported ± the standard deviation.

Surface Wetting

Wilhelmy plate measurements were used to determine the advancing and receding contact angles of polymer-coated coverslips. Two separate trials were performed with three coverslips for each HEMA/EMA composition examined in each trial. Standard 24 mm × 50 mm coverslips (Baxter) were silanized before copolymer application with 2-(3,4 epoxycyclohexyl ethyltrimethoxy silane) for 75, 86, and 100 mol % HEMA and (3-aminopropyltriethoxy silane) for the remainder. Copolymers were applied by slowly dipping the coverslip into a 4% (w/v) polymer solution. Samples were oven dried overnight at 60°C to remove excess solvents and then soaked in water for 24 h to hydrate the films. Contact angles were determined by holding the slide vertically from a microbalance (Fisher) and bringing a water trough up to the sample and measuring the weight of the attached meniscus. Deflections of the microbalance are calibrated with standard weights allowing for a conversion from surface tension to contact angle. Average values of the two trials are reported ± the standard deviation. Details of the apparatus and analysis technique are available.[16]

The capillary rise measurements were performed by clamping a pair of identically prepared IOWs in a parallel-plate configuration with a separation of 0.02 in. between the two waveguide surfaces maintained by precision shims. The two opposing waveguides were set in a trough containing deionized water, and the water meniscus rose up the separation by capillary action. The height of the capillary rise was imaged with a silicon intensified target (SIT) camera against a grid calibrated in mm. The measured rise h is related to the advancing contact angle by $\cos\theta = Kh$,[17] where K is a constant determined by measuring the capillary rise between two hydrophilic glass surfaces of known advancing contact angle, as determined previously by Wilhelmy plate. Unlike Wilhelmy plate measurements, capillary rise has the inherent limitation of not being able to measure contact angles > 90°.

Surface Composition

Copolymer surface compositions were determined by X-ray photoelectron spectroscopy (XPS). Thin films of each polymer were spun cast onto 1-cm^2 silicon wafer sections. The samples were then loaded and scanned in a Perkin–Elmer PHI 5400 XPS spectrometer using a magnesium X-ray source operating at 15 kV at 2×10^{-8} Torr with a 1-mm spot size. Spectra of both the C_{1S} and O_{1S} regions, 284–294 eV and 530–540 eV, respectively, were collected. Survey scans were performed followed by sample dwell times of 15 min at a 45° angle from the normal corresponding to a 50 Å profiling depth. Further analysis at 20° and 70°, corresponding to 20 Å and 100 Å profiling depths, respectively, was also performed on all but the homopolymer samples. Curve fitting to the XPS data were conducted with existing software from Apollo. The ratio of the C=O and

C—O band intensities of the 45° XPS scans were measured and all values were normalized to the C=O/C—O ratio for EMA. According to molecular structure, EMA and HEMA should have C=O/C—O intensity ratios of $\frac{1}{2}$ and $\frac{1}{3}$, respectively. Using C=O/C—O as a variable, the mol % HEMA at the copolymer surface was determined from the linear relationship $100[x/(x + y)] = 300 - 600(C{=}O/C{-}O)$. The XPS measurements were performed by Dr. Richard Linton in the Chemistry Department of the University of North Carolina, Chapel Hill.

Surface Morphology

Backscatter scanning electron microscopy (SEM) was performed on each polymer in a JEOL 1200EX electron microscope to investigate the presence or absence of domain structure within the polymer films. Thin film samples were prepared on Therminox coverslips (Electron Microscopy Sciences) to reduce charging effects and allowed to dry as previously mentioned. Staining of the HEMA moieties at the terminal —OH group (Fig. 1) was performed by exposing the films to osmium tetroxide (OsO_4) vapor for 4 h at 60°C. At this time visible staining had occurred and the samples were removed. Samples were then fixed to carbon SEM stubs and sputter coated with carbon. Sequential backscatter SEM was performed with a tilt of 30° from the normal at magnifications between 100× and 10,000×. The samples were mounted and coated by Dr. Peter Ingram in the Department of Pathology at Duke University. The SEM measurements were performed by Dr. Ingram at the Research Triangle Institute, Research Triangle Park, NC.

Waveguide Characterization

Cleaned quartz substrates, 1″ × 3″ × 5 mm (Hoya), were held by a vacuum chuck in a photoresist spinner (Headway Research) and approximately 1 mL of copolymer solution was applied to the substrate surface. The copolymer-coated slides were spun for 4 min at 1000 RPM, allowed to rest for 2 min, and spun for a final 2 min at 1000 RPM. Waveguides were oven dried and then stored in sealed Coplin jars until used. Transverse electric (i.e., horizontal) polarized laser light at 488 nm or 514.5 nm (Coherent Innova-70) from an argon ion laser was prism coupled (O'Hara, $n_p = 1.85$) into the zeroth order mode of the thin-film IOW. The thickness and refractive index of each waveguide were determined from the coupling angle Φ that propagated guided modes using the eigenvalue equation technique.[18] The dB/cm propagation loss of the waveguides at three locations across the width of the coupling prism was determining by fitting the attenuation of the guided mode intensity to a logarithmic decay. This was achieved by analyzing a digitized image of the waveguide streak directly imaged onto the focal plane of a liquid-nitrogen-cooled charge-coupled device (CCD) camera (Photometrics CE200) fitted with a 50 mm f/2 camera lens (Pentax). Emission spectra of the copolymers were obtained by imaging the guided mode onto the entrance slit (0.2 mm) of a single grating monochromator (Spex 500M) operating as a spectrograph and detecting the wavelength dispersed light with the CCD camera. Monomer spectra were collected from sealed capillaries using the spectrograph. The experimental configuration used for determining the waveguide propagation losses and collecting emission spectra are described in detail elsewhere.[19]

Data Analysis

Correlation coefficients and Student's t-tests of the data were performed in Cricket Software's Statworks. Copolymer reactivity ratios for the free radical copolymerization of two monomers[1] were estimated for HEMA/EMA in Microsoft's Excel by the method of intersection.[20] Both the copolymer equation describing copolymer formation at low conversion[1] and the integrated copolymer equation for high conversions[20] were used in this analysis.

RESULTS

Copolymer Characterization

Table I lists the mol % HEMA in the monomer feed and the resultant percent conversion of monomer to polymer, the percent swelling of polymer in water after 24 h, and the polymer bulk refractive index. Clearly, the degree of copolymerization increased with increasing HEMA content, and as expected, so did the percent swelling and refractive index. Table II presents the mol % HEMA composition of the polymer bulk as measured by transmission IR, and the mol % HEMA at the polymer surface measured to depths of approximately 6000 Å and 50 Å by ATR-FTIR and XPS, respectively. Correlation plots of the transmission IR data with the ATR-IR and XPS data (correlation plots not shown) yielded slopes of 0.89 and 1.06, respectively (t-test of slopes: $p < 10^{-4}$), intercepts insignificantly different than zero (t-test of intercepts: $p > 0.05$), and correlation coefficients of $R^2 = 0.986$ and 0.997, respectively.

Table I Bulk Properties of Homopolymers and Copolymers

Mol % HEMA in Monomer Feed	% Conversion (mols/mols)	% Swelling (wt/wt)	Bulk Refractive Index
100	90	40.8 ± 1.2	1.5297 ± .0028
80	75	25.8 ± 2.9	—
60	73	19.8 ± 2.0	1.5057 ± .0046
40	76	8.8 ± 2.1	1.4931 ± .0005
20	70	7.5 ± 4.4	1.4895 ± .0005
10	69	—	1.4723 ± .0026
0	60	4.9 ± 3.2	1.4685 ± .0008

Therefore, the copolymer bulk is compositionally indistinguishable from the surface.

Figure 2 examines the copolymerization reactions as a function of mol % HEMA in the monomer feed. These data include the total moles of monomer in the monomer feed, the total moles of monomer incorporated into the copolymer, and the moles of each monomer incorporated into the copolymers. Except for the copolymer produced from the 1/9 HEMA/EMA mixture, Figure 2 shows a copolymer that is always richer in HEMA than the monomer feed, and a percent conversion of monomer to copolymer that steadily decreases with decreasing HEMA content of the monomer feed. Therefore it was necessary to allow the reactions to go to high conversion to obtain copolymers with appreciable EMA content, even for EMA-rich monomer feeds (Table II, Fig. 2).

Polymer Morphology

The HEMA homopolymer was most heavily stained by osmium, while the staining of the copolymers was less extensive. The EMA homopolymer was just slightly tinted indicative of some background staining. All SEM images were amorphous and featureless at a resolution of 0.1 μm, suggesting a uniform distribution of osmium-stained HEMA in the copolymers and the HEMA homopolymer. Consistent with the visual appearance of the HEMA/EMA films, backscatter SEM showed no domain structure, surface defects, and/or phase separation in the copolymer series.

Table II Bulk and Surface Composition

Mol % HEMA in Monomer Feed	Mol % HEMA in Polymer		
	Transmission IR[a]	ATR-IR[a]	XPS[b]
100	100	100	106
80	89	—	—
60	86	86	87
40	75	75	82
20	43	43	45
10	10	10	11
0	0	0	0

[a] Measurement based on HEMA homopolymer as 100 mol % HEMA.

[b] Measurement based on EMA homopolymer as 0 mol % HEMA.

Surface Wetting

Table III lists the Wilhelmy plate and capillary rise contact angle measurements as a function of mol % HEMA content of the polymer. Both the advancing and receding contact angles decreased with higher HEMA content of the polymer, while the error in the advancing and receding contact angle measurements both increased with higher HEMA content. Wilhelmy plate and swelling measurements were

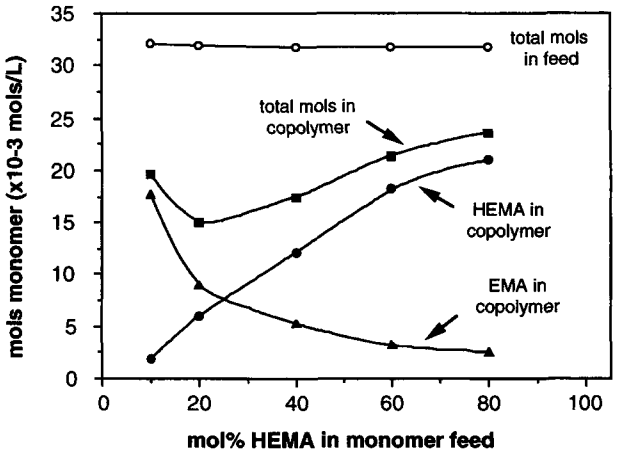

Figure 2 Moles monomer and copolymer in 40-mL reaction mixture before and after 12-h polymerization plotted as a function of mol % HEMA in monomer feed.

Table III Contact Angles of Homopolymers and Copolymers

Mol % HEMA in Polymer	Wilhelmy Plate		Capillary	
	Advancing	Receding	mm Rise	Contact Angle
100	63.3 ± 3.9	26.0 ± 2.3	12	59.8
86	70.7 ± 2.3	40.5 ± 1.2	10	65.2
75	74.7 ± 1.7	40.9 ± 1.6	7	72.9
43	78.8 ± 1.3	58.9 ± 1.4	6	75.4
10	79.7 ± 0.1	62.8 ± 0.1	4	80.3
0	82.2 ± 0.3	70.0 ± 0.7	0	90.0[b]
Hydrophilic glass[a]	15.4 ± 3.9	13.3 ± 6.2	23	15.4

[a] Advancing contact angle used to calibrate capillary rise measurements.
[b] Maximum calculable contact angle by capillary rise.

also attempted on unhydrated polymer films (data not shown). The unhydrated receding contact angle showed essentially the same results as the hydrated films. However, the unhydrated films had advancing buoyancy curves that were too noisy to yield meaningful data. Only the unhydrated EMA homopolymers gave reasonable results for both the advancing and receding contact angles.

The surface energies of the unhydrated polymer films were more reliably characterized by measuring the capillary rise of water between two opposing HEMA/EMA waveguides of identical composition. The capillary rise advancing contact angles of the HEMA/EMA surfaces are also listed in Table III, where a capillary rise for hydrophilic glass was used to calibrate the measurements [i.e., $\theta_{adv} = \cos^{-1}[(h/23)\cos(15.4°)]$]. Note that the EMA homopolymer had a capillary rises of 0 mm that corresponds to the maximum measurable contact angle of 90°.

Like the Wilhelmy plate measurements of the hydrated polymer surfaces, the capillary rise contact angles of the unhydrated polymer surfaces decreased with increasing HEMA content ($R^2 = 0.890$). The only obvious discrepancy between the capillary rise and Wilhelmy plate advancing contact angles is the EMA homopolymer that became markedly more wettable after 24 h soaking in water. Neglecting the EMA homopolymer (for which accurate capillary rise data was not obtained), correlation of the advancing contact angles for the hydrated and unhydrated polymers yielded a slope of 1.19 ± 0.17 (t-test of slope: $p < 0.05$) and an intercept not statistically different than zero (t-test of intercept: $p > 0.05$). Therefore the surface energies of the hydrated polymers appeared to be just slightly lower than the unhydrated polymers.

Optical Characterization

Table IV lists the waveguide characterization data for the HEMA/EMA polymers. Few, if any scattering sites were visible in the films and all waveguides efficiently guided light as evidenced by the low propagation losses of < 1 dB/cm, where 1 dB/cm is the benchmark figure for a "good" thin film IOW.[21] The waveguide thickness and refractive index decreased and increased, respectively, with increasing HEMA content of the waveguide. The refractive index is a direct consequence of the waveguide HEMA/EMA composition, while the decreasing waveguide thickness was simply a matter of the polymer solution viscosity that decreased with increasing HEMA content (i.e., a less viscous polymer solution resulted in thinner waveguides when spun cast into films on the substrate surface).

Emission from the $m = 0$ guided mode of each waveguide was collected from 3250 to 1000 cm^{-1} to examine the background emission of the waveguides (data not shown). Raman bands were observed for

Table IV Characterization of HEMA/EMA Copolymer IOWs

Mol % HEMA in Polymer	Thickness (μm)	Refractive Index	Propagation Loss (dB/cm)
100	0.93	1.520	0.59 ± 0.09
86	1.06	1.500	0.89 ± 0.09
75	1.36	1.487	0.39 ± 0.07
43	1.85	1.476	0.52 ± 0.02
10	2.30	1.472	0.45 ± 0.03
0	2.80	1.468	0.78 ± 0.05

the methyl stretching at 2940 cm^{-1} that is exclusive to EMA, and the carbonyl band at 1435 cm^{-1} that is common to both HEMA and EMA. These bands were superimposed on a broad fluorescence background across the entire collection region that increased with HEMA content of the waveguide. Transmission Raman spectra of the liquid HEMA and EMA monomers showed the optical grade HEMA monomer was considerably more fluorescent than the EMA monomer, suggesting the likely source of the polymer fluorescence background.

Correlation of Measured Properties to Polymer Composition

Figure 3 plots the Wilhelmy plate, swelling, and refractive index data in Tables I, III, and IV against the mol % of HEMA in the polymer bulk. The straight lines represent the linear fits that correlated best to the data. The refractive index and the advancing and receding contact angles were all fit significantly by a single straight line (R^2 = 0.838 for waveguide refractive index; R^2 = 0.878 for bulk refractive index; R^2 = 0.841 for advancing contact angle; R^2 = 0.944 for receding contact angle; t-test of all slopes and intercepts: $p < 0.05$), while the 24-h swelling data would not fit a single line with any degree of confidence (R^2 = 0.606; t-test of slope and intercept: $p > 0.05$). However, it is apparent that the refractive index and percent swelling remain relatively unaffected by copolymer compositions until 75 mol % HEMA, after which both parameters increased sharply. Consequently, these data sets are better fit by discontinuous lines with a near zero slope for HEMA contents $\leq$ 75 mol % (R^2 = 0.989 for swelling; R^2 = 0.962 for waveguide refractive index; and R^2 = 0.997 for bulk refractive index) and a steeper slope for HEMA contents of $\geq$ 75 mol % (R^2 = 0.985 for swelling; R^2 = 0.996 for waveguide refractive index; and R^2 = 0.988 for bulk refractive index).

The advancing and receding contact angles of the HEMA/EMA polymers also correlated well with the composition of the polymer surfaces as determined by XPS (t-test of slopes and intercepts: $p < 0.05$), with the correlation being stronger for the receding angle (R^2 = 0.950) than for the advancing angle (R^2 = 0.835). However, since the copolymer compositions determined by transmission IR and XPS are virtually identical these data are redundant with Figure 3(a) and are not presented. Nonetheless, the magnitudes of advancing and receding contact angles decreased with increasing HEMA content of the polymer. In addition, the hysteresis between advancing and receding angle increased with the HEMA content of the copolymer. This is expected because the advancing and receding contact angles are more influenced by the hydrophobic and hydrophilic character of the surface, respectively.[22]

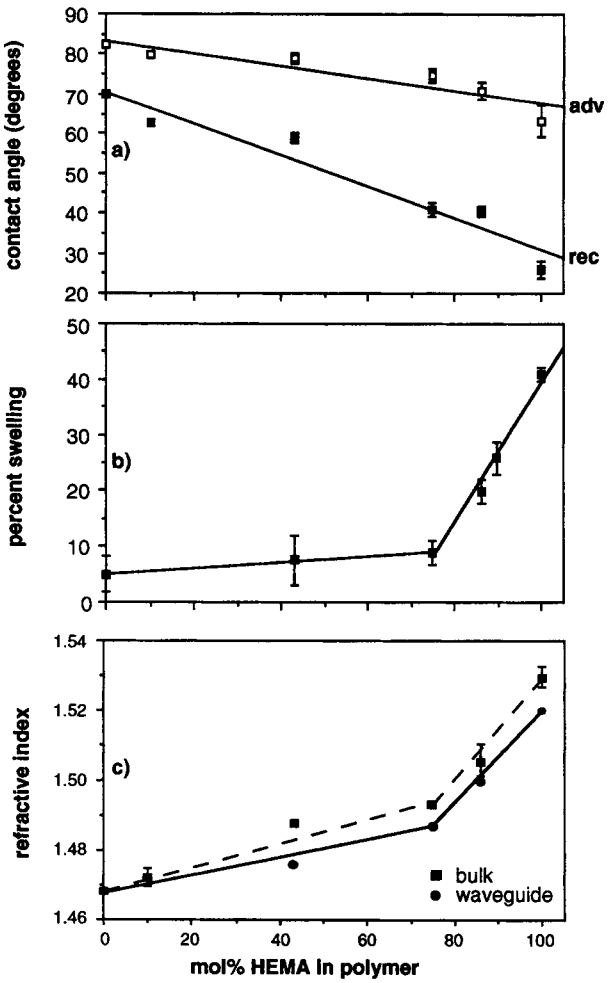

Figure 3 Combined plots of (a) Wilhelmy plate contact angles, (b) % swelling, and (c) refractive index plotted as a function of mol % HEMA in the polymer film. The straight lines are the best linear fits to the data. Note that the Wilhelmy plate data were well fit by a single straight line, but the swelling and refractive index data were better fit by discontinuous lines.

DISCUSSION

This paper presents the fabrication and characterization of a HEMA/EMA copolymer series used to make thin-film IOWs by spin casting. HEMA and

EMA homopolymers and copolymers were fabricated by thermally initiated free radical polymerization of dilute monomer solutions. Polymers were characterized: physically by their bulk and surface copolymer composition, bulk swellability, and surface wettability; and optically by their waveguide thickness, refractive index, propagation losses, and emission background.

With the exception of copolymer containing 10 mol % HEMA, all of the synthesized copolymers were richer in HEMA than the monomer feed, and the percent conversion of monomer to copolymer increased steadily with increasing HEMA in the monomer feed (Tables I, II, and Fig. 2). These observations are consistent with a copolymerization of HEMA and EMA monomers having significantly different reactivities. From the manufacturers' Q and e values for HEMA and EMA (Rohm & Haas), reactivity ratios of $r_1 = 1.34$ and $r_2 = 0.74$, for HEMA and EMA respectively, are estimated.[1] Similarly, the copolymer equations produced $r_1 = 1.85$, $r_2 = 0.24$ for low conversion and $r_1 = 1.00$, $r_2 = 0.43$ for high conversion.

HEMA/EMA films initially fabricated from ethanol and toluene solvents were cloudy and contained visible regions of phase separation that were completely unacceptable as waveguides. This necessitated using a new solvent system of DMF for polymers from HEMA-rich monomer feeds and a mixture of isobutanol/toluene for EMA-rich monomer feeds. HEMA/EMA films cast from these solvents were clear, macroscopically homogeneous, and visually defect free. The apparent lack of phase-separated polymers was supported by back scatter SEM measurements showing a homogeneous distribution of osmium-stained HEMA moieties in the copolymers down to the 0.1-μm scale.

The advancing and receding contact angles measured by Wilhelmy plate of samples soaked for 24 h in water showed a linear gradient of increased surface wettability with increasing HEMA content of the polymer (Table III), ranging from moderately hydrophobic EMA ($\theta_{adv} = 82°$, $\theta_{rec} = 70°$) to moderately hydrophilic HEMA ($\theta_{adv} = 63°$, $\theta_{rec} = 26°$). The equilibrium or static contact angles of the unhydrated polymer surfaces measured by capillary rise (Table III) correlated strongly with the advancing angles measured for the hydrated polymers, again ranging from hydrophobic EMA ($\theta_{adv} = 90°$) to moderately hydrophilic HEMA ($\theta_{adv} = 60°$). The only truly dissimilar surface was the EMA homopolymer that appeared to become significantly less hydrophobic upon hydration. Advancing and receding contact angles of the hydrated surfaces also correlated well with the composition of the unhydrated polymer surfaces as determined by XPS.

Combined, these data suggest that the polymer surfaces were similar in the hydrated and unhydrated states. However, the Wilhelmy plate advancing buoyancy curves were erratic for all of the unhydrated surfaces except for the EMA homopolymer, whereas all hydrated surfaces gave well-behaved results (Table III). This indicates to the contrary that the polymer surfaces became significantly different upon hydration. The most likely explanation for this discrepancy is that the Wilhelmy plate is a nonequilibrium measurement that was sensitive to the difference between hydrated and unhydrated HEMA moieties,[22] and capillary rise is a static measurement that was less sensitive to this effect.

Consistent with their visual appearance, spun cast HEMA/EMA waveguides exhibited low propagation losses between 0.5 and 0.9 dB/cm (Table IV). The measured waveguide refractive index range of 1.520–1.468 (Table IV) was very close to the polychromatic bulk refractive indices ranging from 1.523 for HEMA to 1.469 for EMA [Table I, Fig. 3(c)]. Both the waveguide refractive index and percent swelling increased minimally for waveguides of $\leq$ 75 mol % HEMA, but rose sharply for waveguides with HEMA contents of $>$ 75 mol % HEMA [Fig. 3(b,c)]. The origin of this discontinuity is presumably related to a critical composition of HEMA necessary to produce marked changes in the optical and swelling properties of the copolymers.

Emission spectroscopy of the copolymer IOW waveguides yielded vibrational spectra complementary to IR analysis. However, the intensity of the Raman bands was swamped by the fluorescence of the copolymers: that is, the background fluorescence increased with mol % HEMA in the copolymer, with the Raman bands of the HEMA homopolymer being barely detectable. Because HEMA and EMA are themselves nonfluorescent, this points out that the ppm impurity levels of optical grade HEMA and EMA are unacceptable for waveguide spectroscopic applications.[19] This problem is being addressed by removing the MEHQ stabilizer from both monomers by ion exchange. Although our applications lie in the blue-green region of the spectrum, the fluorescence could be avoided altogether by using higher wavelengths such as the 632.8 nm from a HeNe laser.

CONCLUSIONS

Polymer thin-film waveguides were fabricated from a structurally homologous series of HEMA/EMA

copolymers that present a gradient of optical, bulk swelling, and surface wetting properties. Waveguides produced from these polymers appeared to be optically homogeneous and defect free with low dB/cm propagation losses. The measured bulk and surface properties of the polymers strongly correlated with their monomer composition, and the surface composition of the polymers were virtually identical to the bulk. These results indicate the relative HEMA/EMA content was primarily responsible for the observed gradient of properties. However, the swelling and refractive index of the copolymers showed a discontinuity of properties at high EMA content, and the Wilhelmy plate results suggest that the hydrated and unhydrated copolymer surfaces were different. Although some inhomogeneities in the copolymer waveguides may have existed; no phase separation of the copolymers was observed by SEM on a 0.1-μm scale, and the waveguides efficiently guided light.

This work was supported by NIH Grant HL 32132. Appreciation is extended to A. Lyter and R. Linton of the University of North Carolina, Chapel Hill for performing the XPS analysis; P. Ingram of the Research Triangle Institute for performing the backscatter SEM measurements; D. Gregonis of Ohmeda, Salt Lake City, and H. Clark of Duke University for helpful discussions on the polymer synthesis; and M. Garrison of Duke University for his assistance in the waveguide measurements.

REFERENCES

1. F. Rodriguez, *Principles of Polymer Systems,* Hemisphere Publishing, New York, 1989.
2. M. Ruben, *Color Atlas of Contact Lenses & Prosthetics,* 2nd ed., C. V. Mosby Company, St. Louis, 1989.
3. R. Jeyanthi and K. P. Rao, *J. Bioactive Compatible Polym.,* **5,** 194 (1990).
4. M. Stol, I. Cifkova, V. Tyrackova, and M. Adam, *Biomaterials,* **12,** 454 (1991).
5. A. D. Andrade, *Hydrogels for Medical and Related Applications, ACS Symposium Series 31,* American Chemical Society, Washington, D.C., 1976.
6. Y. C. Ko, B. D. Ratner, and A. S. Hoffman, *J. Coll. Interf. Sci.,* **82,** 25 (1981).
7. T. A. Horbett, J. J. Waldburger, B. D. Ratner, and A. S. Hoffman, *J. Biomed. Mater. Res.,* **22,** 383 (1988).
8. I. A. Feuerstein, W. G. McClung, and T. A. Horbett, *J. Biomed. Mater. Res.,* **26,** 221 (1992).
9. T. A. Horbett, *J. Biomed. Mater. Res.,* **15,** 673 (1981).
10. D. S. Walker, M. D. Garrison, and W. M. Reichert, *J. Coll. Interf. Sci.,* **157,** 41 (1993).
11. P. K. Tien, *Appl. Optics,* **10,** 2395 (1971).
12. J. T. Ives and W. M. Reichert, *J. Appl. Polymer Sci.,* **36,** 429 (1988).
13. J. F. Rabolt, R. Santo, N. E. Schlotter, and J. D. Swalen, *IBM Res. Dev.,* **26,** 209 (1982).
14. D. S. Walker, Masters thesis, Duke University, Dept. of Biomedical Engineering, 1992.
15. T. A. Horbett, M. B. Schway, and B. D. Ratner, *J. Coll. Interf. Sci.,* **104,** 28 (1985).
16. M. D. Garrison, Masters thesis, Duke University, Dept. of Biomedical Engineering, 1992.
17. P. C. Hiemenz, *Principles of Colloid and Surface Chemistry,* 2nd ed., Marcel Dekker, New York, 1986.
18. P. W. Bohn, *Anal. Chem.,* **57,** 1203 (1985).
19. D. S. Walker, C. J. Berry, and W. M. Reichert, *Appl. Spect.,* **46,** 1437 (1992).
20. R. F. Mayo and F. M. Lewis, *J. Am. Chem. Soc.,* **66,** 1594 (1944).
21. J. D. Swalen, R. Santo, M. Tacke, and J. Fischer, *IBM J. Res. Dev.,* March, **21,** 168 (1977).
22. J. D. Andrade, *Surfaces and Interfacial Aspects of Biomedical Polymers,* Vol. 2, Plenum Press, New York, 1985.